Numerical Simulation of Flow Over Different Types of Airfoils

Conference Paper · January 2020

CITATIONS
2

READS
2,822

3 authors:

Neslihan Aydın
Uludag University
16 PUBLICATIONS **7** CITATIONS
SEE PROFILE

Mehmet Erman Çalışkan
Uludag University
10 PUBLICATIONS **46** CITATIONS
SEE PROFILE

Irfan Karagoz
Uludag University
60 PUBLICATIONS **1,018** CITATIONS
SEE PROFILE

Numerical Simulation of Flow Over Different Types of Airfoils

Neslihan Aydın[*], Mehmet Erman Çalışkan[*], İrfan Karagöz[#]

[*] *Department of Mechanical Engineering, Uludag University, Bursa, Turkey,16059*
nslhngunes@uludag.edu.tr

[#] *Department of Mechanical Engineering, Uludag University, Bursa, Turkey,16059*
karagoz@uludag.edu.tr

***Abstract*— Airfoils in various types are widely used in many devices subjected to fluid flows such as aircraft, vehicles, turbines, etc. Therefore, analyzing the fluid flow around an airfoil is one of the important subjects in fluid mechanics. In this study, the conservation equations of two-dimensional compressible flow over standard aerofoils were solved by using different numerical techniques. After a mesh independence study, applied mathematical model, numerical methods and obtained results are confirmed with experimental results given in the literature. Three different turbulence models, namely the k-ω, the Spalarat Almaras and Reynolds stress models were used in the solutions. The performances of turbulence models were evaluated under the results obtained. The verified numerical model was also applied to the flow over different types of blades, including a special airfoil design. Velocity and pressure fields obtained around these airfoils were analysed, and their aerodynamic performances in terms of the lift and drag coefficients were compared to each other at different angles of attack.**

***Keywords*— renewable energy, computational fluid dynamics, airfoils, turbulence models, lift and drag coefficients.**

I. INTRODUCTION

Since energy is indispensable for human beings, research works are underway on especially renewable energy sources such as solar energy, wind energy, and hydroelectric energy. One of the most widely used renewable energy types is wind energy in which energy is generally obtained by means of wind turbines. One of the parts to be considered in the design of the turbine is blade. The airflow around the turbine blades affects the amount of energy production. Therefore, the velocity of the airflow around an airfoil and profile shapes have been investigated by many researchers.

Recently, flow phenomena passing through solids have been an important research subject due to aerodynamic effects such as lifting and drag on solid bodies. Especially in airfoil design, different shape airfoil profiles and their aerodynamic effects have been an important research subject.

Among the studies, bio-inspired wing designs are noteworthy. Başak & Demirhan (2017) were inspired by the fins of the humpback whales, and they developed tubercled airfoil design. As a result they found that the tubercled airfoil increased efficiency by approximately 42.09 % compared to normal airfoil design at the speed of 100 m/s [1]. Another experimental and numerical study was performed on the flow around NACA 0015 airfoil design at angles of attack ranges from 2 to 18º. Numerical results were obtained by using different turbulences models which are Spalart Allmaras and k-epsilon. They found that the best results for lift and drag coefficient were obtained 16º attack angle [2]. A numerical simulation aimed to analyze the aerodynamic characteristics of NACA0012 airfoil was carried out by a researcher who focused on the designing a airfoil with better aerodynamic performance. NACA 0012 and the turbulence flow structure were tested in detail with the Large Eddy Simulation Model for different attack angles [3]. The flow behaviour over AG-16 airfoil was studied and analysed numerically by researchers, aerodynamic performance of AG-16 airfoil at different angles of attack ranging from 0 degree to 15 degree was obtained using ANSYS-FLUENT software. They found that the maximum lift coefficient for high lift airfoil type AG-16 recorded at 0.0116 and the drag coefficient magnitude was equal to 0.0013 when the angle of attack reached the stall limit [4]. A numerical study was performed with k-ω shear stress transport model (SST Model) for turbulence intensities of 1% and 5%. NACA 0012 airfoil subjected to different flap angles and Mach number. They calculated lift coefficients (C_L), drag coefficients (C_D) and C_L/C_D ratio at different operating conditions and showed that with increasing Mach number (M) C_L increases but C_D remains somewhat constant [5]. Matyushenko et al. investigated numerically and experimentally airfoils with different shapes and thicknesses at high Reynolds numbers ($Re \geq 10^6$)and low turbulence intensity ($I \leq 0{,}1\%$) using two-dimensional Reynolds-Averaged Navier-Stokes equations (RANS) closed by different turbulence models. Results show that comparison with the corresponding data for the γ-SST model; both models are unable to predict the dependence of the lift coefficient on the angle of attack [6]. Holden et al. investigated the design of wind turbine blade that inspired by maple seed in their study. As a result of the study biomimetic wind turbine airfoil maple seed profile Cp power coefficient increased to a maximum value of 0,59. They also reached C_L value up to 0,8 for maximum Re=10000 [7].

II. TURBULENCE MODELS

In order to examine the velocity and pressure distributions in a flow field, the conservation of mass and momentum equations must be solved under the existing boundary conditions [8]. However, it is difficult and even impossible to define these conservation equations in complex geometries and solve them analytically. Therefore, equations must be solved numerically.

According to Newton's law, the motion of a viscous fluid is defined by the Navier-Stokes equations in differential form. Navier-Stokes equations formulize the differential form of conservation of momentum [9]. Incompressible Navier-Stokes equations in Cartesian coordinates are expressible as follows;

$$x-direction = \frac{\partial u}{\partial t} + u\frac{\partial u}{\partial x} + v\frac{\partial u}{\partial y} + w\frac{\partial u}{\partial z} = -\frac{1}{P}\frac{\partial P}{\partial x} + g_x + v\left(\frac{\partial^2 u}{\partial x^2} + \frac{\partial^2 u}{\partial y^2} + \frac{\partial^2 u}{\partial z^2}\right) \quad (1)$$

$$y-direction = \frac{\partial v}{\partial t} + u\frac{\partial v}{\partial x} + v\frac{\partial v}{\partial y} + w\frac{\partial v}{\partial z} = -\frac{1}{P}\frac{\partial P}{\partial y} + g_y + v\left(\frac{\partial^2 v}{\partial x^2} + \frac{\partial^2 v}{\partial y^2} + \frac{\partial^2 v}{\partial z^2}\right) \quad (2)$$

$$z-direction = \frac{\partial w}{\partial t} + u\frac{\partial w}{\partial x} + v\frac{\partial w}{\partial y} + w\frac{\partial w}{\partial z} = -\frac{1}{P}\frac{\partial P}{\partial z} + g_z + v\left(\frac{\partial^2 w}{\partial x^2} + \frac{\partial^2 w}{\partial y^2} + \frac{\partial^2 w}{\partial z^2}\right) \quad (3)$$

The continuity equation is based on the principle of conservation of mass in control volume, and can be written in differential form as follows;

$$\frac{\partial \rho}{\partial t} + \frac{\partial(\rho u)}{\partial x} + \frac{\partial(\rho v)}{\partial y} + \frac{\partial(\rho w)}{\partial z} = 0 \quad (4)$$

By assuming constant density in equations (1), (2), (3) and (4); the unknown terms are pressure and velocity components and in the x, y and z directions. By solving these four equations, these four unknowns value can be obtained. On the other hand, the Navier-Stokes equations cannot be solved analytically without any simplification. The flow problem is defined within the numerical solution and the result is obtained for each discrete point under specified boundary and initial conditions. However, the Navier- Stokes equations need to be modified in order to take into account turbulence and adopt turbulence models. The Reynolds-Averaged Navier-Stokes (RANS) equations are obtained for this purpose.

A. *Reynolds-Averaged Navier- Stokes Equations RANS*

In these equations, flow properties are separated into two components: time-averaged and time-varying parts. The Navier-Stokes equations are rearranged using this principle and Reynolds Averaged Navier-Stokes (RANS) equations are obtained. Time resolved RANS equations are called as Time-Dependent Reynolds Averaged Navier- Stokes (URANS) equations. Continuity equation (5) and URANS equations (6) respectively can be written as:

$$\frac{\partial \rho}{\partial t} + \frac{\partial}{\partial x_i}(\rho u_i) = 0 \quad (5)$$

$$\frac{\partial}{\partial t}(\rho u_i) + \frac{\partial}{\partial x_j}(\rho u_i u_j) = -\frac{\partial \rho}{\partial x_i} + \frac{\partial}{\partial x_j}\left[\mu\left(\frac{\partial u_i}{\partial x_j} + \frac{\partial u_j}{\partial x_i} - \frac{2}{3}\delta_{ij}\frac{\partial u_i}{\partial x_j}\right)\right] + \frac{\partial}{\partial x_j}\left(-\rho\overline{u_i' u_j'}\right) \quad (6)$$

Here u_i is velocity components and $\left(-\rho\overline{u_i' u_j'}\right)$ indicates Reynolds turbulence stresses. Due to the chaotic nature of turbulence there is no analytical method for calculating these values. Turbulence models are used to calculate the turbulence stresses in the momentum equation. Turbulence models have been developed to calculate these values.

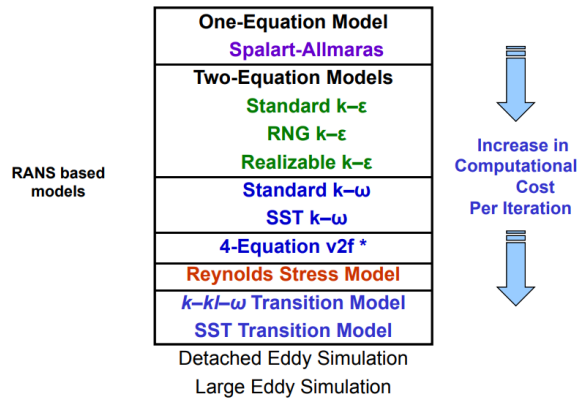

Fig 1. Turbulence models used in ANSYS [10].

B. *Spalart-Allmaras Model*

This model is a one equation model for turbulent viscosity and it solves just one transport equation for viscosity; Spalart-Allmaras is a low-cost RANS model solving a transport equation for a modified eddy viscosity. In particular, it gives good results in the flow around the wall in the boundary layer. Turbomachinery has started to gain popularity in applications [11,12].

$$\frac{\partial}{\partial t}(\rho\hat{v}) + \frac{\partial}{\partial x_j}(\rho\hat{v}u_i) = G_v + \frac{1}{\sigma_{\hat{v}}}\left[\frac{\partial}{\partial x_j}\left[\left\{(\mu + \rho\hat{v})\frac{\partial\hat{v}}{\partial x_j}\right\} + C_{b2}\rho\left(\frac{\partial\hat{v}}{\partial x_j}^2\right)\right]\right] - Y_v \quad (7)$$

In equation (7); $\hat{v}$ turbulence kinematic viscosity, G_v turbulence production, Y_v turbulence destruction; $\sigma_{\hat{v}}$ and C_{b2} indicate constants.

C. *Standard k-ε Model*

K-ε turbulence model is the most common model used in Computational Fluid Dynamics (CFD) to simulate mean flow characteristics for turbulent flow conditions. It is a two equation model which gives a general description of turbulence by means of two transport equations [13].

The standard k-ε turbulence model ; Launder and Spalding, 1974 is used which is based on our best understanding of the relevant processes, therefore minimizing unknowns and presenting a set of equations which can be applied to a large number of turbulent applications [14].

For turbulent kinetic energy (k);

$$\frac{\partial(\rho k)}{\partial t}+\frac{\partial(\rho k u_i)}{\partial x_i}=\frac{\partial}{\partial x_j}\left[\mu_t\frac{\sigma_k}{\partial x_j}\right]+2\mu_t E_{ij}E_{ij}-\rho\epsilon \quad (8)$$

For dissipation (**ε**);

$$\varepsilon=\nu\overline{\frac{u_i'}{\partial x_k}\frac{u_i'}{\partial x_k}} \quad (9)$$

Where; ui represents velocity component in corresponding direction, Eij represents component of rate of deformation, μij represents eddy viscosity.

D. Standard k- ω Model (WİLCOX Model)

The other common and simplest model is k-ω model. It provides better modeling of the turbulent boundary layer than the standard k-ε model, however is more sensitive to the free-stream turbulence levels [15]. Given the processes of convection, diffusion and destruction or dissipation, the model equation for ω is given below:

$$\rho\frac{\partial\omega}{\partial t}+\rho U_j\frac{\partial\omega}{\partial x_j}=\frac{\partial}{\partial x_j}\left((\mu+\sigma\mu_t)\frac{\partial\omega}{\partial x_j}\right)+P_\omega-D_\omega \quad (10)$$

The model attempts to predict turbulence by two partial differential equations for two variables, k and ω, with the first variable being the turbulence kinetic energy (k) while the second (ω) is the specific rate of dissipation of the turbulence kinetic energy (k).

$$P_\omega=\alpha\frac{\omega}{k}\tau_{ij}\frac{\partial U_i}{\partial x_j}=\alpha\frac{\omega}{k}P_k \quad (11)$$

$$D_\omega=\beta\rho\omega^2 \quad (12)$$

E. Reynolds Stress Equation Model (RSM)

Reynolds stress equation model (RSM), also known as second order or second moment closure model is the nearly most complex classical turbulence model. Several shortcomings of k-ε turbulence model were observed when it was attempted to predict flows with complex strain fields or substantial body forces. Calculation time is longer than other turbulence models, but keep in sight the lack of isotropic turbulence. The Reynolds averaged momentum equations for the mean velocities are:

$$\frac{\partial U_i}{\partial t}+\frac{\partial(\rho u_i u_j)}{\partial x_j}-\frac{\partial}{\partial x_j}\left[\mu\left(\frac{\partial U_i}{\partial x_t}+\frac{\partial U_j}{\partial x_i}\right)\right]=-\frac{\partial p''}{\partial x_i}-\frac{\partial(\rho\overline{u_i u_j})}{\partial x_j}+S_{M_i} \quad (13)$$

Where p'' is a modified pressure, S_{M_i} is the sum of body forces and the fluctuating Reynolds stress contribution is $-\rho\overline{u_j u_i}$.

RSM needs more modelling. It is more difficult to convergence. Strong streamline curves are suitable for complex 3D streams with swirl and rotation.

III. GEOMETRY AND MESH DESIGN PARAMETERS

A. Geometry Design

Naca 0015 airfoil profile that shown in Fig. 2. was used in the analysis. This profile's data files were taken from airfoiltools.com and geometry was designed on Solidworks 2018 as a 3d.

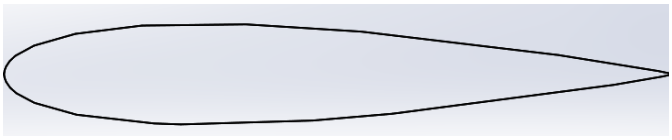

Fig. 2. Naca 0015 airfoil profile

For dimensions of Naca 0015 profile, Robert E. and friend's (1981) paper was used for reasonable compare. Dimension of Naca 0015 airfoil that used in this paper were shown in Fig. 3.

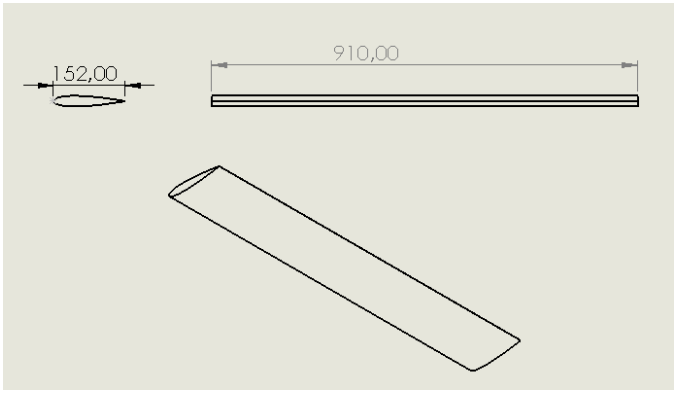

Fig. 3. Dimensions of Naca 0015 airfoil profile (units are mm)

A computational flow domain must be covered this Naca 0015 airfoil profile. There are many flow domain types that used in numerical analysis.

In this study, C type geometry was used as a flow domain (Fig. 4.). Because C type mesh structure allows to create less mesh. Also C type domain is more convenient to create a real flow area.

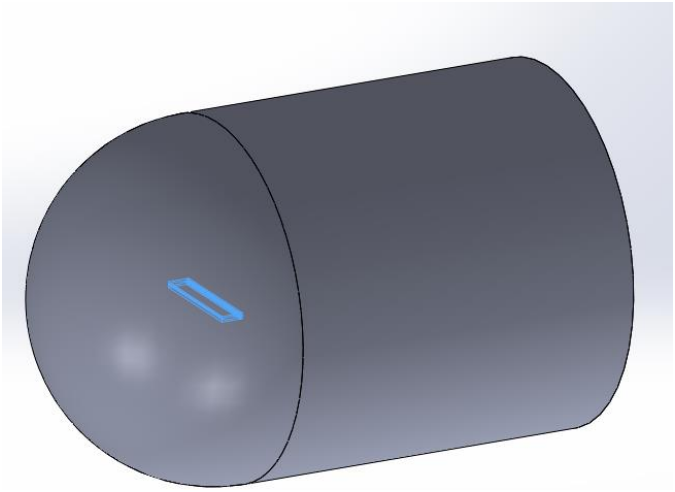

Fig. 4. C type geometry that was designed.

Ansys fluent tutorials was used to determine the sizes of flow areas. Ansys fluent tutorials lectures suggest 10x chord length between air inlet and center of naca profile. Also it suggests 20x chord length between air outlet and center of naca airfoil profile (Fig. 5.).

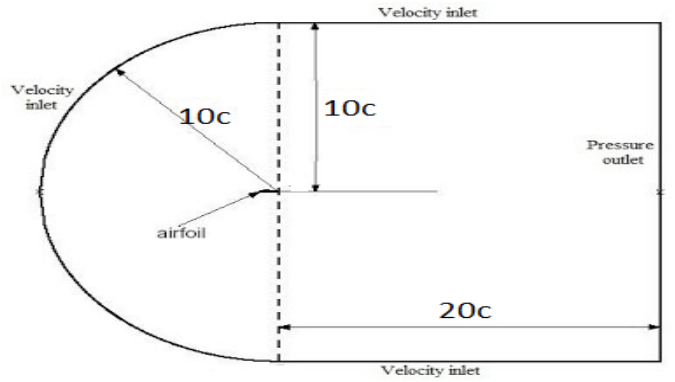

Fig. 5. Certain distances about the c type geometry

Flow domain was subdivided into a series of region. The purpose of this, to create different sized mesh in different regions. Thus, it was able to create finer meshes around the airfoil. The regions on geometry are shown in Fig.6.

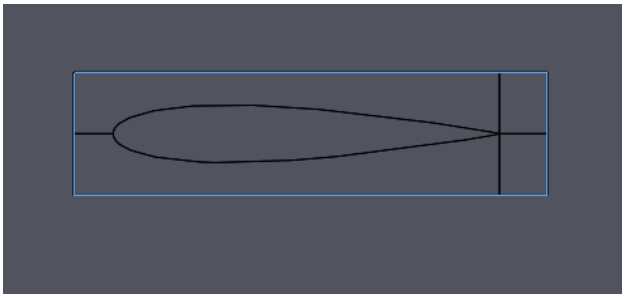

Fig. 6. Different regions on flow domain geometry.

B. Mesh Generation

Mesh generation was made on HYPERMESH 13.0. In order to ensure the desired mesh thickness around the airfoil, different sized mesh structure was generated in different parts of the flow domain geometry. This is done to keep the magnitude of Y-plus as small as possible. The mesh structure created was shown in Fig. 7. from different views.

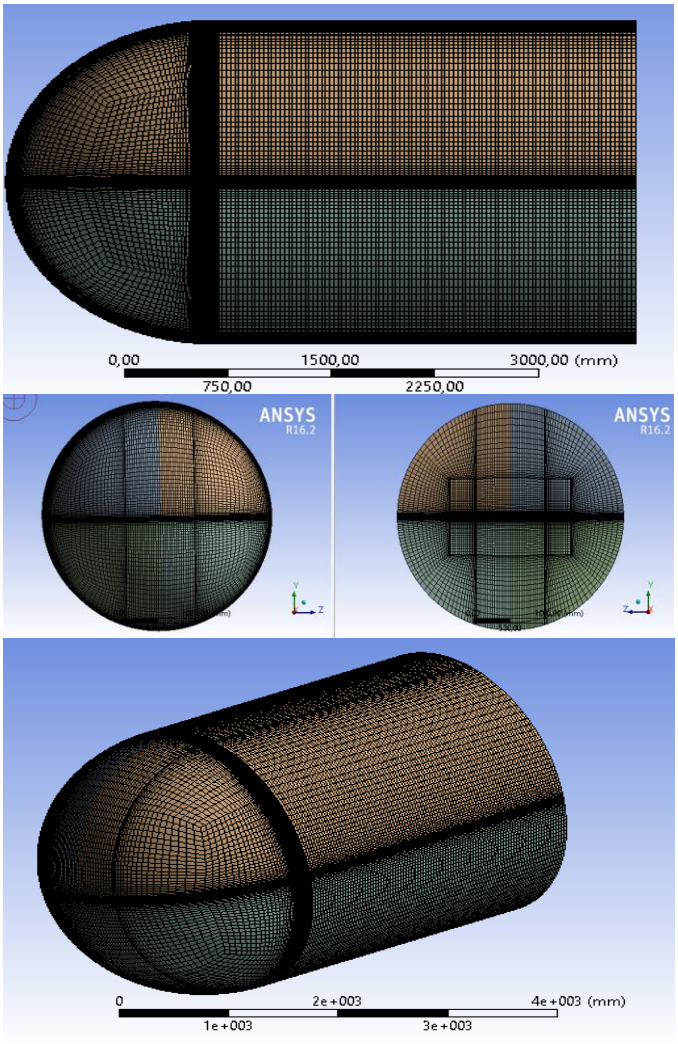

Fig. 7. Different views of mesh structure.

Also, fine mesh structure around the airfoil is seen in Fig. 8. in detail. This view was created by middle section of flow domain.

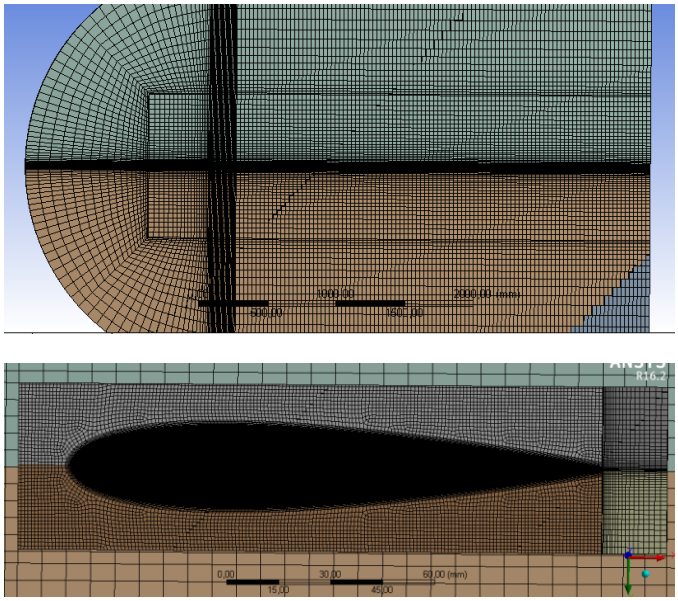

Fig. 8. Section view of mesh structure.

The flow domain is formed by hexa mesh structure. This mesh structure's number of elements is 9533632 and number of nodes 10059476 (Fig. 9.). When creating this mesh structure, 2d mesh structure was created. 3d mesh structure was then generated by these 2d mesh structure.

Statistics	
Nodes	10059476
Elements	9533632
Mesh Metric	None

Fig. 9. Number of nodes and elements of mesh structure.

C. Set up of Analysis

For numerical analysis of Naca 0015 airfoil, ANSYS 16.2 and 17.1 fluent was used. During the analysis, the effect of several parameters on the lift and drag coefficient of the this airfoil was examined.

For this, certain setups have been made on the program. For solution type, Pressure-Based and Steady Type have been used in the analysis.

The inlet of air was adjusted as shown in the Fig. 5. Magnitude of air inlet velocity, was determined to make the Reynolds number of 40000. So magnitude of inlet velocity was determined as a 4.71m/s.

The attack angles were also adjusted in this section to examine the performance of the airfoil at certain attack angles (Fig. 10.).

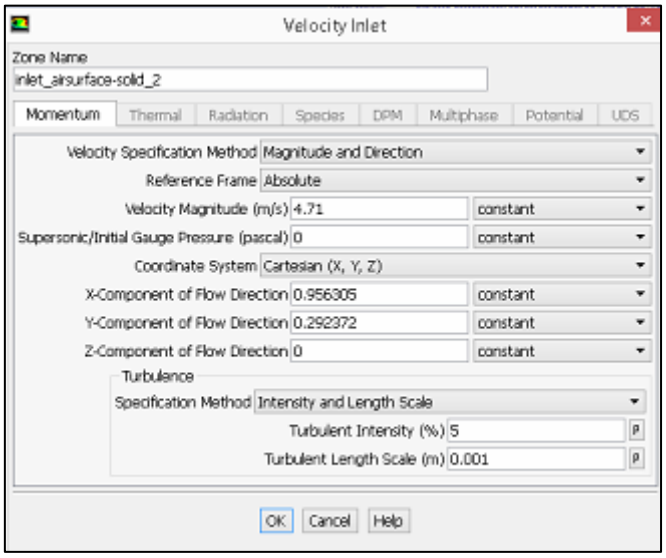

Fig. 10. Setup of the velocity inlet

Determined values for the reference values were shown in Fig. 11. Area value from these values, was calculated by multiplying the chord length with the airfoil z length (0.152*0.91). The length value was taken as the chord length of 0.152 m.

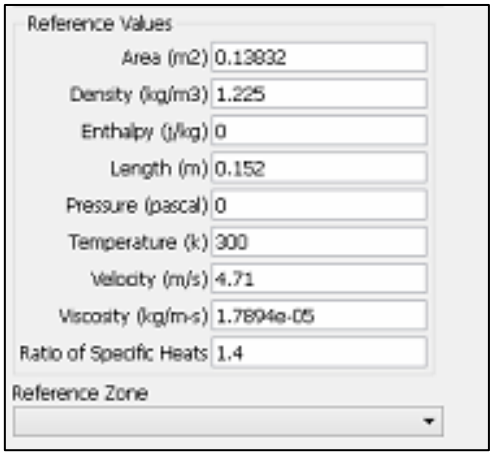

Fig. 11. Reference values

For the solution method, The Simple scheme was used. Also other values were given in Fig. 12. in detail.

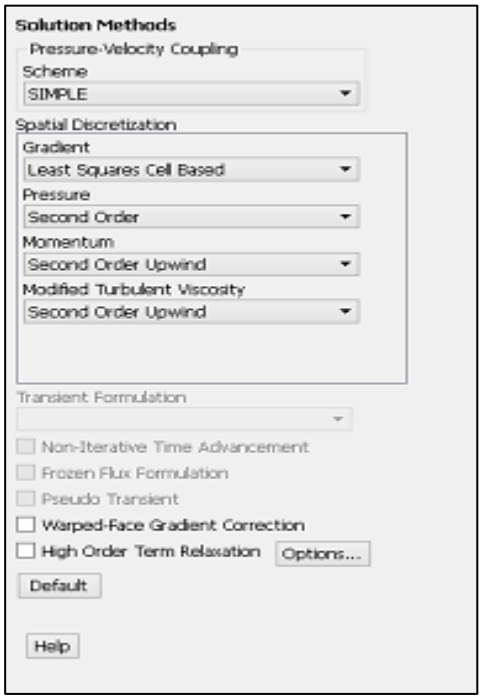

Fig. 12. Setup of solution method

For Cd (drag coefficient) and Cl (lift coefficient) calculation, certain angle values must be written on the x and y component locations on monitors section in program. How these angle values were calculated was shown in the Fig. 13. and Fig. 14.

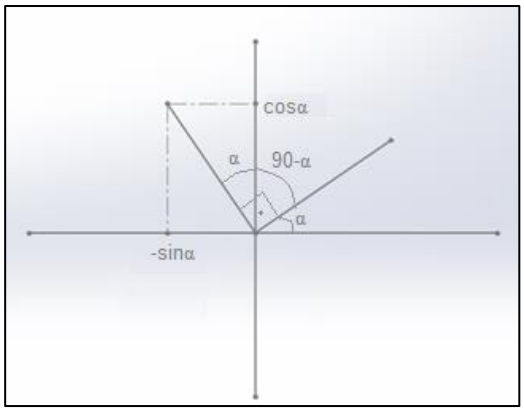

Fig. 13. Vectors of Cl components; calculation of Cl

As shown in the Fig. 14., direction must be normal to flow or perpendicular to drag. So mainstream velocity vector must be stated by 90°.

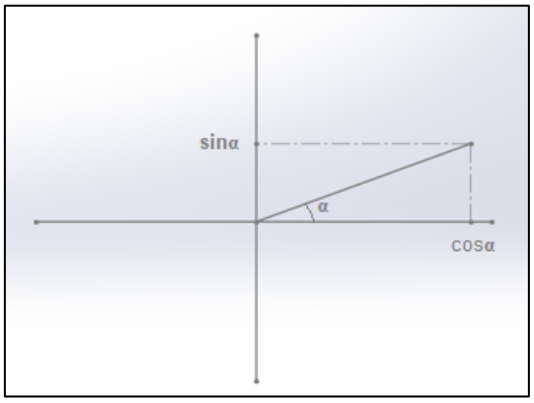

Fig. 14. Vectors of Cd components calculation of Cd

As shown in the Fig. 14., direction must be same as flow, aligned with chord line or attack angle.

IV. RESULTS

In the analysis, firstly, the Cl and Cd coefficients of the Naca 0015 airfoil were examined, with 7° attach angle and Re number of 40000, by using different turbulence models. These results were compared with the experimental data set in the study of Robert et al. (1981) and turbulence model which gives the best results was determined (TABLE I).

TABLE II

COMPARISON OF C_L AND C_D COEFFICIENTS ACCORDING TO TURBULENCE MODELS AT 7° ATTACK ANGLE AND 40000 RE NUMBER

	TURBULENCE MODEL	Cl	Cd
1	Spalart Almaras	0,48543	0,038633
2	k-ε (Realizable)	0,43315	0,053946
3	k-ω (SST)	0,46362	0,037405
4	k-ω (Standart)	0,46825	0,037019
	Experimental Data	0,5730	0,0267

As can be seen from the TABLE III, Spalart Almaras model is the most suitable model.
The results obtained from the Spalart Almaras model, with 7° attack angle and 40000 Re number, were examined.

A. Scaled Residuals

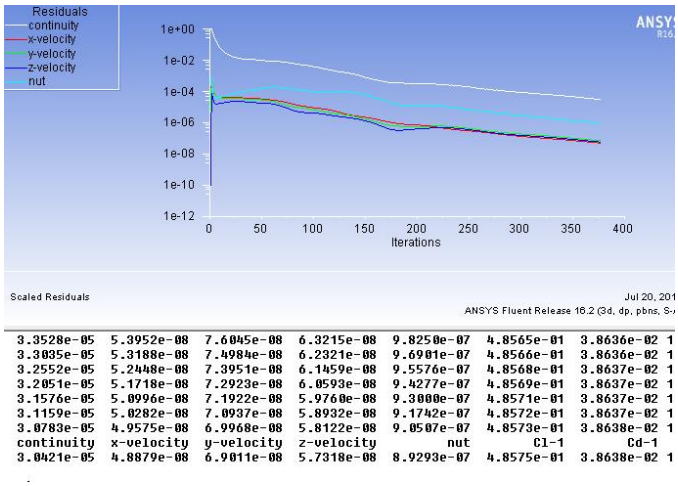

3.3528e-05	5.3952e-08	7.6045e-08	6.3215e-08	9.8250e-07	4.8565e-01	3.8636e-02 1
3.3035e-05	5.3188e-08	7.4984e-08	6.2321e-08	9.6901e-07	4.8566e-01	3.8636e-02 1
3.2552e-05	5.2448e-08	7.3951e-08	6.1459e-08	9.5576e-07	4.8568e-01	3.8637e-02 1
3.2051e-05	5.1718e-08	7.2923e-08	6.0593e-08	9.4277e-07	4.8569e-01	3.8637e-02 1
3.1576e-05	5.0996e-08	7.1922e-08	5.9760e-08	9.3000e-07	4.8571e-01	3.8637e-02 1
3.1159e-05	5.0282e-08	7.0937e-08	5.8932e-08	9.1742e-07	4.8572e-01	3.8637e-02 1
3.0783e-05	4.9575e-08	6.9968e-08	5.8122e-08	9.0507e-07	4.8573e-01	3.8638e-02 1
continuity	x-velocity	y-velocity	z-velocity	nut	Cl-1	Cd-1
3.0421e-05	4.8879e-08	6.9011e-08	5.7318e-08	8.9293e-07	4.8575e-01	3.8638e-02 1

Fig. 15. Scaled residuals of number 1 analysis in the TABLE IV

As can be seen from Fig.15. , convergence curves are sufficiently reduced.

B. Yplus Values

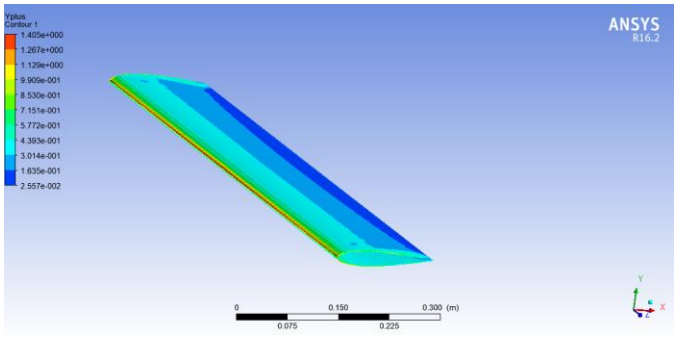

Fig. 16. Y plus values of number 1 analysis in the TABLE I

Yplus value is often used to describe how coarse or fine a mesh is for a particular flow pattern. In the airfoil analysis, Yplus value should be examined on the airfoil. Usually this Yplus value is required max value 1. Therefore, the mesh thickness around the airfoil, which is shown in detail in the Fig. 8, was reduced to 0.05 mm.
As can be seen from the Fig.16., the max y plus value on the airfoil was obtained from the analysis is 1,405.

C. Pressure Contours

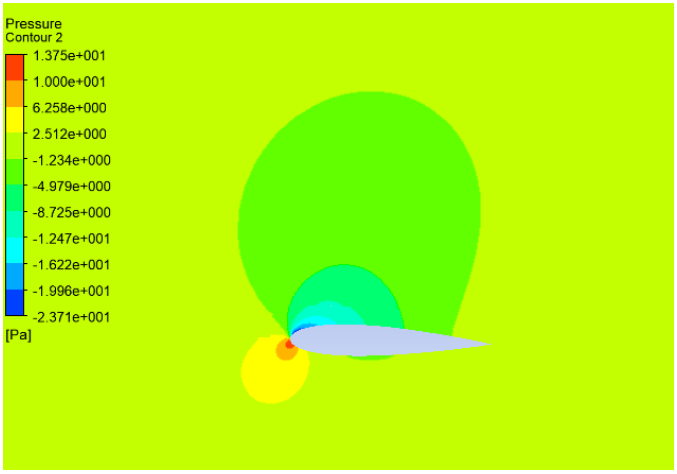

Fig. 17. Pressure contour of number 1 analysis in the TABLE V

The high pressure at the bottom inlet of the airfoil has increased up to 13,75Pa. In the upper part of the airfoil, because of the high velocity, the pressure has dropped to -23,71Pa. When the pressure contours are examined, it is seen that the pressure distribution around the airfoil develops regularly.

D. Velocity Contours

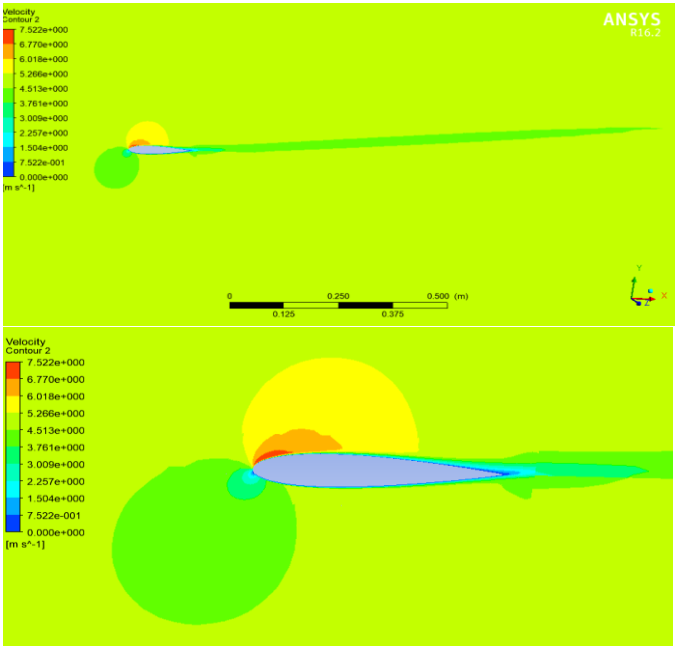

Fig. 18. Velocity contour of number 1 analysis in the TABLE VI

As can be seen in the Fig.18, a wake region was formed in the rear part where the air is separated from the airfoil. This wake area was about 1 meter long. Air flowed slightly slower than the inlet velocity in the wake region

E. Velocity Vectors

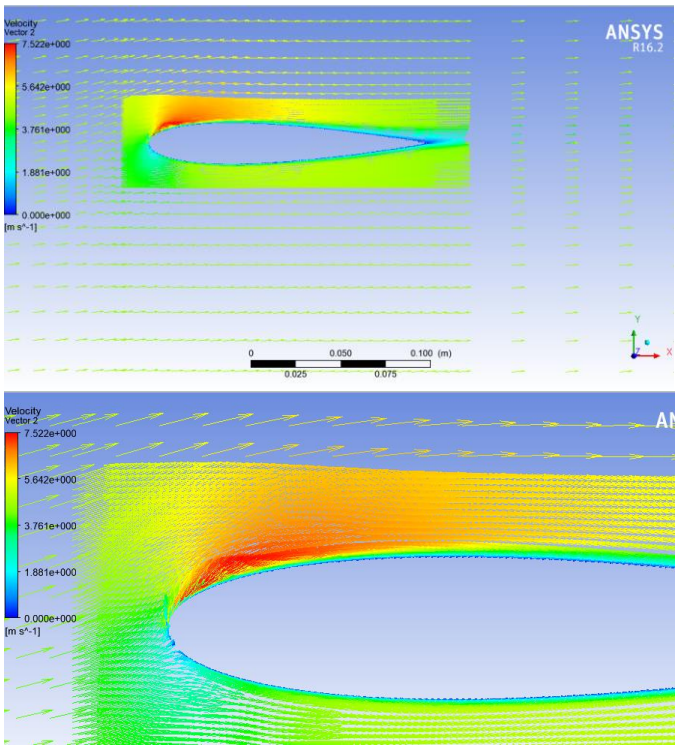

Fig. 19. Velocity vector of number 1 analysis in the TABLE VII

When air velocity vectors are considered, it is seen that air velocity increases up to 7,52 m/s in upper parts of airfoil after entering air.

F. Investigation of NACA 0015 AİRFOİL performance according to attack angle

After determining the most suitable turbulence model, C_L and C_D coefficients were examined according to attack angle with 40000 Re number. The results obtained from these analyses between 5° and 18° attack angles are presented in the Fig.1 and TABLE II.

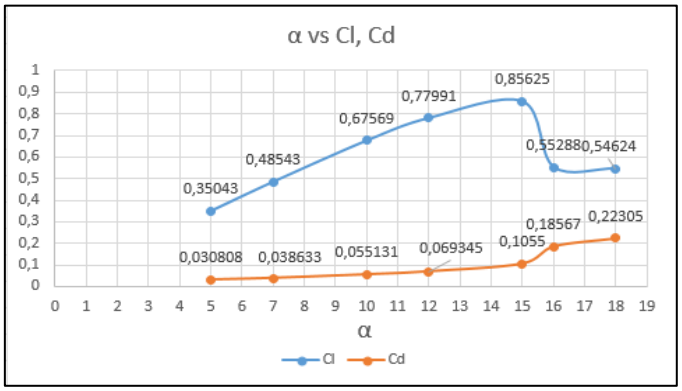

Fig. 20. $C_L$and C_d values of Naca0015 Airfoil according to attack angle with 40000 Re number.

TABLE II
C_L AND C_D VALUES OF NACA 0015 AIRFOIL ACCORDING TO ATTACK ANGLE WITH RE NUMBER 40000

α	Cl	Cd	Cl/Cd
5	0,35043	0,030808	11,37464
7	0,48543	0,038633	12,56516
10	0,67569	0,055131	12,25608
12	0,77991	0,069345	11,24681
15	0,85625	0,1055	8,116114
16	0,55288	0,18567	2,977756
18	0,54624	0,22305	2,448958

There is a stall angle where the coefficient of C_L starts to decrease while the angle of attack increases. As can be seen from the Fig.20, this stall angle is 15° for this analysis. Also, the highest ratio of C_L/C_D was observed at 7°.

V. CONCLUSIONS

In this paper, NACA0015 Airfoil are investigated with different turbulence methods; k-ε, k-ω, k-ω (SST) models.

- The Spalart-Allmaras model provided C_L and C_D values in the best agreement with experimental results. This model is generally recommended for flow analysis over airfoils [2].
- In addition, k-ω models have been shown to provide good results for flow analysis over the airfoil.
- C_D value increased with attack angle but C_L value was initially increasing with attack angle after a stagnation point these was called as a stall angle or stall point C_L decreased critically. In this study stall angle was obtained as 15°.
- The performance of any airfoil is measured with the C_L/C_D ratio. The highest ratio of C_L/C_D was observed at 7°.
- The max y plus value on the airfoil was obtained from the analysis is 1,405. Considering that the

max yplus value should be 1, this result was considered acceptable.

References

[1] H. Başak , H. Demirhan , Examination of Airfoil Profile Yield Inspired by The Fins of Humpback Whale with CFD Analysis , Journal of Gazi Engineering Sciences, 2017, 3(2):15-20.

[2] I. Şahin, A. Acir, Numerical and Experimental Investigation of Lift and Drag Performances of NACA0015 Wind Turbine Airfoil, IJMMM 2015 Vol.3(1): 22-25 ISSN: 1793-8198.

[3] L.B. Streher, , "Large-eddy simulations of the flow around a NACA0012 airfoil at different angles of attack",Physics, Fluid Dynamics thesis, Helmut-Schmidt-Universitat der Bundeswehr, Hamburg, May 2017.

[4] A. H. Mutaib, A. AL-Khateeb, M. K. Khashan, F. Kamil, Computational Study of Flow Characteristics Over High Lift Airfoil at Various Angles of Attack, Journal of Mechanical Engineering Research & Developments (JMERD) 42(1) (2019) 90-9.

[5] T. Ahmed, Md. T. Amin, S.M. R. Islam, S. Ahmed, Computational Study of Flow Around a NACA 0012 Airfoil Flapped at Different Flap Angles with Varying Mach Numbers, Global Journal of Researches in Engineering General Engineering Vol.13(4)(2013):5-16.

[6] A. A. Matyushenko, E. V. Kotov, A. V. Garbaruk, Calculations of Flow Around Airfoils Using Two Dimensional RANS: An Analysis of the Reduction in Accuracy,St. Petersburg Polytechnical University Journal: Physics and Mathematics Vol.3(4) (2017):15-21.

[7] J. Holden, T. M. Caley, M. G. Turner, Maple Seed Performance as a Wind Turbine, Conference: AIAA SciTech 2015, At Kissimmee, FL, Volume: AIAA 2015-1304. DOI: 10.2514/6.2015-1304.

[8] Y. A. Çengel, J. M. Cimbala, Solutions Manual for Fluid Mechanics: Fundamentals and Applications Second Edition, McGraw-Hill, 2010.

[9] B. Apaçoğlu, "Cfd Analyses of Uncontrolled and Controlled Laminar and Turbulent Flows Over A Circular Cylinder", Mechanical Engineering Master thesis, TOBB University of Economics and Technology,Ankara 2010.

[10] ANSYS FLUENT 13.0 Lecture 06 Turbulence User Guide,2013.

[11] P.R.Spalart, S.R. Almaras, A One-Equation Turbulence Model for Aerodynamic Flows. 1992. AIAA Paper 92-0439.

[12] H. B. Ekmekci, "Modification Of A Computational Fluid Dynamics Model (Ansys-Fluent) For The Purpose Of River Flow And Sediment Transport Modeling", Master of Science in Civil Engineering Thesis, The Graduate School of Engineering and Sciences of İzmir Institute of Technology, İzmir, July, 2015.

[13] F.Kaya, İ. Karagöz, Investigation into the Suitability of Turbulence Models in Swirling Flows, Uludag University Journal of The Faculty of Engineering Vol 12(1) (2007):85-96.

[14] B.E. Launder, D.B. Spalding, The Numerical Computation of Turbulent Flows. Computer Methods in Applied Mechanics and Engineering, 3, (1974) 269-289.

[15] D.C. Wilcox, Turbulence Modeling for CFD. 2006, DCW Industries, Inc.

[16] R. E Sheldahl, P. C. Klimas, Aerodynamic characteristics of seven symmetrical airfoil sections through 180-degree angle of attack for use in aerodynamic analysis of vertical axis wind turbines (No. SAND-80-2114). Sandia National Labs., Albuquerque, NM (USA). (1981).